ELSEVIER

Journal of Quantitative Spectroscopy & Radiative Transfer 106 (2007) 325–347

Journal of Quantitative Spectroscopy & Radiative Transfer

www.elsevier.com/locate/jqsrt

# Past, present, and future of global aerosol climatologies derived from satellite observations: A perspective

Michael I. Mishchenko[a,*], Igor V. Geogdzhayev[b], Brian Cairns[b], Barbara E. Carlson[a], Jacek Chowdhary[b], Andrew A. Lacis[a], Li Liu[b], William B. Rossow[a], Larry D. Travis[a]

[a]*NASA Goddard Institute for Space Studies, 2880 Broadway, New York, NY 10025, USA*
[b]*Columbia University, 2880 Broadway, New York, NY 10025, USA*

**Abstract**

A number of passive satellite instruments have been used to develop global climatologies of terrestrial tropospheric aerosols by analyzing the properties of sunlight reflected by the atmosphere–surface system. The outcome of these efforts are several climatologies which all purport to represent the same aerosol characteristics such as optical thickness and size. However, the quantitative differences between these climatologies have been found to far exceed the corresponding individual uncertainty claims. The magnitude of these differences is alarming and necessitates a detailed critical assessment and integrated analysis that would go far beyond simple intercomparisons of various satellite products and comparisons of satellite aerosol optical thickness results with ground-based sun-photometer data. This paper outlines the framework for a global long-term satellite climatology of aerosol properties based on a consistent combination of previous, current, and near-future satellite retrievals. We also discuss potential future strategies for deriving a much improved aerosol climatology from Earth-orbiting satellites.
Published by Elsevier Ltd.

*Keywords:* Tropospheric aerosols; Remote sensing

*Abbreviations:* AERONET, aerosol robotic network; ALIVE, aerosol lidar validation experiment; AOT, aerosol optical thickness; APS, aerosol polarimetry sensor; ATSR, along track scanning radiometer; AVHRR, advanced very high resolution radiometer; CALIPSO, cloud-aerosol lidar and infrared pathfinder satellite observations; CLAMS, Chesapeake lighthouse and aircraft measurements for satellites; CRYSTAL-FACE, cirrus regional study of tropical anvils and cirrus layers—Florida area cirrus experiment; CSTRIPE, coastal STRatocumulus imposed Perturbation experiment; EOS, Earth observing system; GACP, global aerosol climatology project; GCM, global circulation model; GEWEX, global energy and water cycle experiment; GHG, greenhouse gas; GOME, global ozone monitoring experiment; IFOV, instantaneous field of view; IHOP, international $H_2O$ Project; INTEX-B, phase B of intercontinental chemical transport experiment—north America; ISCCP, international satellite cloud climatology project; MILAGRO, megacity initiative: local and global research observations; MISR, multiangle imaging spectroradiometer; MODIS, moderate-resolution imaging spectroradiometer; MTI, multispectral thermal imager; NASA, national aeronautics and space administration; NOAA, national oceanic and atmospheric administration; OMI, ozone monitoring instrument; POES, polar operational environmental satellites; POLDER, polarization and directionality of the Earth's reflectance instrument; RSP, research scanning polarimeter; SAGE, stratospheric aerosol and gas experiment; SCIAMACHY, scanning imaging absorption spectrometer for atmospheric chartography; SNR, signal-to-noise ratio; SSA, single-scattering albedo; SWIR, short-wave infrared; TOMS, total ozone mapping spectrometer; VIIRS, visible infrared imager/radiometer suite

*Corresponding author. Tel.: +1 212 678 5590; fax: +1 212 678 5552.
*E-mail address:* mmishchenko@giss.nasa.gov (M.I. Mishchenko).

0022-4073/$ - see front matter Published by Elsevier Ltd.
doi:10.1016/j.jqsrt.2007.01.007

## 1. Introduction

Tropospheric aerosols are believed to cause a significant forcing of climate comparable to that of the GHGs, but the magnitude of this forcing still remains highly uncertain because of inadequate quantitative knowledge of global aerosol characteristics and their temporal changes [1–7]. This is illustrated in Fig. 1 based on a recent study by Hansen et al. [8]. Black carbon aerosols absorb the solar energy and then re-radiate it at infrared wavelengths, thereby causing positive radiative forcing and contributing to global warming. Sulfate particles and other nonabsorbing aerosols reflect the solar radiation back to space and thus cause atmospheric and surface cooling. Besides these direct interactions of aerosols with radiation, aerosols cause an indirect cooling effect by modifying cloud-radiative properties and modulating precipitation. It is seen that the estimated magnitude of the cumulative aerosol forcing and its current uncertainty are comparable to those of the sum of all climate forcings.

The analyses by Hansen et al. [8,9] as well as the other recent studies referenced above imply that the uncertainty in the aerosol climate forcing remains unacceptably large and must be reduced by at least a factor of 3 [10]. Achieving this goal requires a comprehensive aerosol-monitoring program (e.g., [11]) with three major science objectives shown in the left-hand panel of Fig. 2 (cf. [12]). The right-hand panel of Fig. 2 lists the minimal set of aerosol and cloud parameters that must be retrieved from space with a passive remote-sensing instrument in order to facilitate the accurate quantification of the aerosol effects on climate. The corresponding measurement accuracy requirements are dictated by the need to detect changes of the aerosol radiative forcing estimated to be possible during the next two decades and to determine quantitatively the contribution of this forcing to the planetary energy balance [13].

A number of passive satellite instruments have been used to retrieve global distributions of tropospheric aerosol properties (e.g., [14]), most notably the AVHRR instruments on the NOAA POES platforms, TOMS [15], GOME [16,17], SeaWiFS [18], POLDER [19], MODIS [20], MISR [21], MTI [22], ATSR [23,24], OMI [25], and SCIAMACHY [26]. The outcome of these efforts are several global climatologies (e.g., [15,27–32]) which all purport to represent the same aerosol characteristics such as optical thickness $\tau$ and size. It may thus appear that combining these products into a unified long-term aerosol climatology spanning the past three decades would be a rather straightforward procedure. However, it is becoming increasingly obvious that the quantitative differences between the individual satellite climatologies on both the local and the global scale and over both short and long time periods far exceed the corresponding individual uncertainty claims.

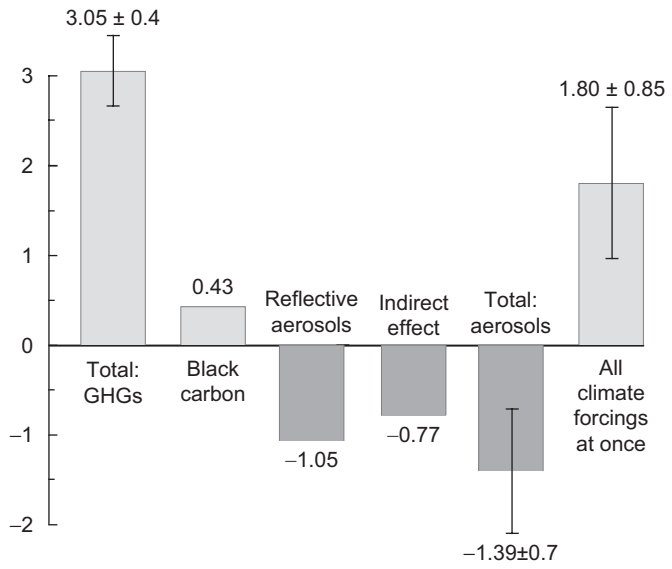


Fig. 1. Estimated changes in select climate forcings (in $W/m^2$) during the period 1880–2003.

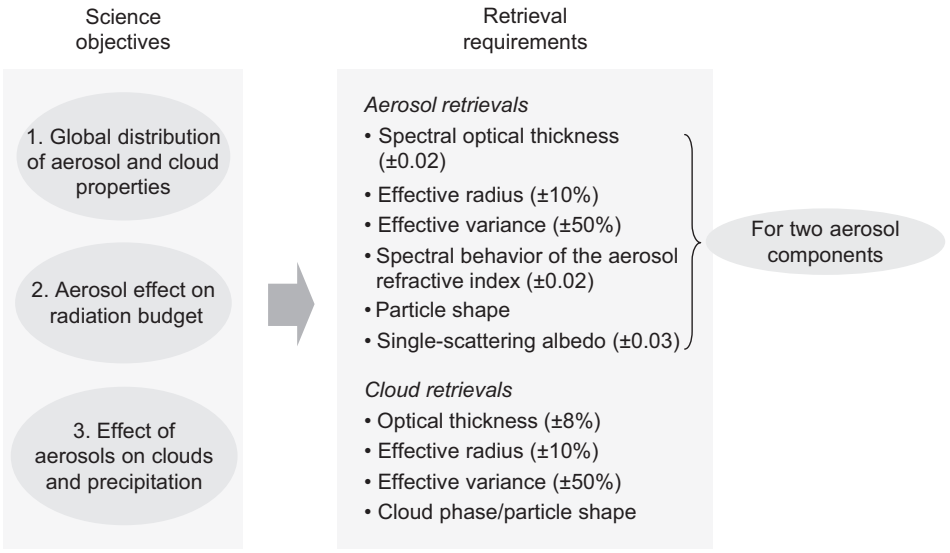


Fig. 2. Objectives of a comprehensive aerosol monitoring program and the corresponding passive retrieval requirements.

This is well illustrated by Fig. 3, which shows seasonal AOT distributions obtained by averaging the results accumulated over the entire duration of the respective datasets (with the exception of AVHRR/GACP, in which case the periods affected by the El Chichon and Mt. Pinatubo eruptions were excluded). It is commonly believed that accurate AOT retrievals are significantly easier than those of any other aerosol characteristic. Therefore, the large amount of averaging used to compute each seasonal AOT value in Fig. 3 was expected to yield nearly identical results for the advanced MODIS and MISR retrievals. However, it is seen that the residual differences are quite significant and greatly exceed the maximal margin of uncertainty dictated by the ultimate task to quantify the direct and indirect aerosol forcings. These differences in the seasonal AOT averages are especially surprising in view of the recent publications documenting successful validations of daily MODIS and MISR AOTs against the benchmark AERONET results (e.g., [31,32]).

Similarly, Fig. 4 shows significant differences in the aerosol Ångström exponent averaged over 45°S–45°N and over all available data of the respective instruments. The Ångström exponent is easier to retrieve than the particle size distribution [27], yet the differences are large even for the same type of instrument (MODIS) but flown on different platforms (Terra and Aqua). It goes without saying that the differences in the individual daily retrievals of the AOT and Ångström exponent can be expected to be much greater than those in Figs. 3 and 4. Greater still differences can be expected for the other aerosol characteristics listed in the right-hand panel of Fig. 2.

Whereas the AVHRR aerosol products are based on low-quality radiance datasets and can only be expected to become better as the result of comparisons with the newer MODIS and MISR products, the large quantitative differences between the latter are alarming and necessitate a detailed critical assessment and integrated analysis. The results of the previous studies (e.g., [31,32,34–42]) suggest that the requisite analysis must go far beyond simple intercomparisons of various satellite products and comparisons/validation of satellite AOTs with/against the AERONET data. The former reveals the differences but do not help to identify their causes, whereas the latter systematically appear to involve too much human selectivity as well as a priori information not contained in the operational satellite products (e.g., the presence of undetected clouds in the satellite instrument IFOV).

It is now well recognized that the ability of a satellite instrument to provide accurate aerosol and cloud particle characteristics is constrained by the following factors.

(i) the extreme complexity of the atmosphere–surface system reflecting sunlight towards the spacecraft,
(ii) the need to characterize this system by a large number of model parameters and retrieve all of them simultaneously,

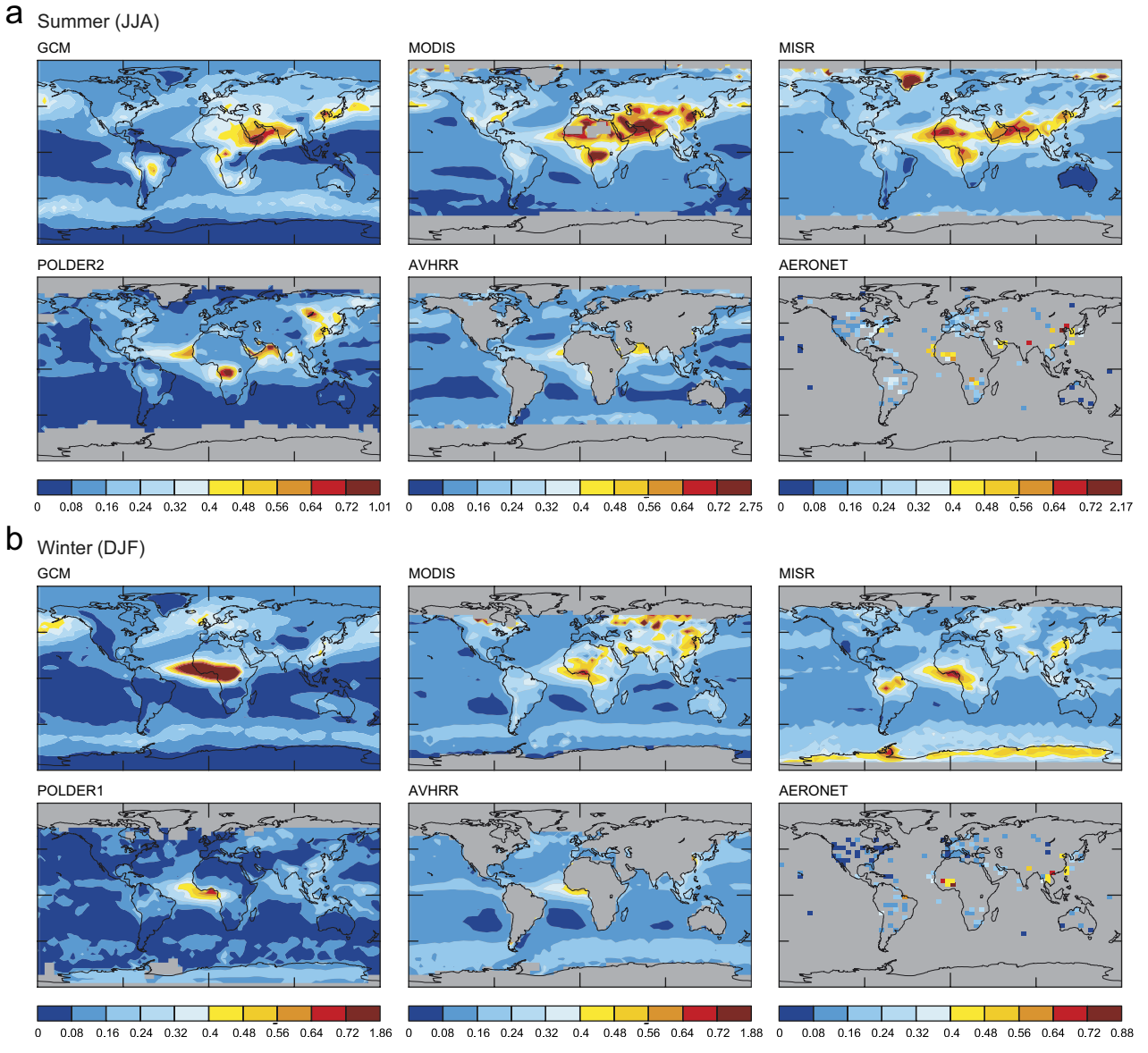


Fig. 3. Overall seasonal means of AOT at 550 nm compiled from MODIS, MISR, POLDER, AVHRR (GACP), and AERONET datasets as well as modeled with the GISS GCM. The color bars are evenly scaled, except the right end numbers, which represent the maximum value for each column (after [33]).

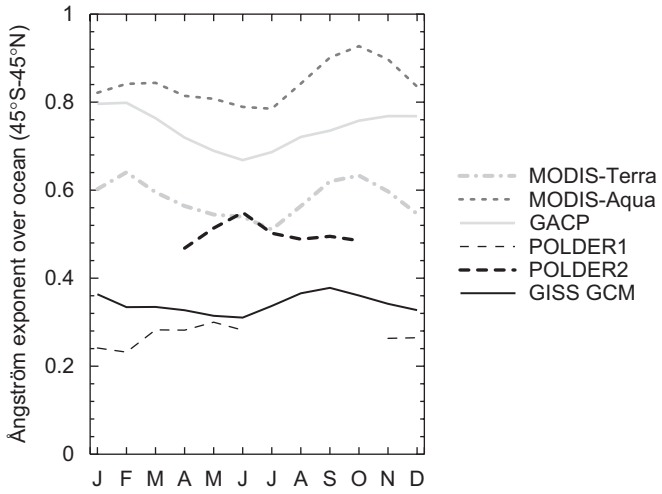


Fig. 4. Seasonal dependence of area-weighted overall monthly mean Ångström exponent over the oceans from different data sources. The results have been computed by averaging over 45°S–45°N and over all available data of the respective instruments.

(iii) the strong temporal and spatial variability of aerosol and cloud fields,
(iv) the significant diversity of aerosol particle morphologies, sizes, and compositions,
(v) the frequent co-existence of different aerosol types,
(vi) the occurrence of partially cloudy pixels, and
(vii) the presence of optically thin cirrus clouds.

The number of unknown model parameters often exceeds the number of independent pieces of data provided by a satellite measurement for a given scene location. The retrieval procedure then yields a range of model solutions all of which are equally acceptable since they all reproduce the measurement data equally well within the measurement errors [43,44].

The only way to ameliorate the ill-posed nature of the inverse retrieval problem is to increase the number of independent pieces of data per scene until it significantly exceeds the number of unknown model parameters. Only then the retrieval procedure based on a minimization technique is likely to become stable and yield a unique solution.

The potential information content of data provided by a passive satellite instrument measuring the reflected sunlight can be increased by:

(i) measuring not only the intensity, $I$, but also the other Stokes parameters describing the polarization state of the reflected radiation (i.e., $Q$, $U$, and $V$; [45–48]),
(ii) increasing the number of well-separated spectral channels and widening the total spectral range covered,
(iii) increasing the number and range of viewing directions from which a scene location is observed, and
(iv) improving the measurement accuracy.

Therefore, a (near) ultimate passive instrument for aerosol remote sensing from space would have the following characteristics (cf. [13,43,44,49–52]):

(i) the ability to measure all Stokes parameters (or at least $I$, $Q$, and $U$),
(ii) high photometric (a few percent) and polarimetric ($\sim$0.1%) accuracy and precision,
(iii) multiple ($\gtrsim$10) narrow spectral channels (for both intensity and polarization) providing a representative sampling of a wide spectral interval ranging at least from $\sim$400 to $\sim$2200 nm,
(iv) views of each scene location from multiple ($\gtrsim$20) directions,
(v) a small geometric IFOV ($\sim$2 km), and

(vi) a wide (~2000 km) swath providing global coverage every two days (assuming a sun-synchronous polar orbit).

For various technical and logistical reasons, such an instrument neither exists nor is planned. Furthermore, it may even be impossible to design and build (see Section 7). Therefore, the current strategy for developing a unified satellite climatology of aerosol properties has to rely on data from less capable yet existing (or soon-to-be-flown) instruments. Given the complexity of the underlying problem and the limited retrieval capabilities offered even by state-of-the-art instruments, this task appears to be extremely difficult and requires innovative solution approaches.

The main purpose of this paper is to outline what we believe is a feasible framework for the development of a unified long-term aerosol climatology. Our approach is based on a thorough critical assessment, integrated analysis, and consistent combination of datasets acquired with previous and current satellite instruments as well as with instruments expected to be launched in the near future. In the development of this framework, we have relied on our extensive experience gained through the analysis and interpretation of the AVHRR and RSP data. These two instruments may be thought of representing, respectively, the bottom and the top of the hierarchy of passive aerosol remote-sensing tools, with all other instruments occupying intermediate positions. On one hand, the AVHRR dataset has been a constant reminder of how challenging it is to retrieve aerosol properties from space. On the other hand, by sub-setting the RSP dataset and disabling parts of the RSP retrieval algorithm one can model and analyze in detail the performance of essentially any passive satellite instrument. This analysis tool becomes critically important when it comes to creating a unified aerosol climatology using data from real rather than ideal instruments.

## 2. Description of instruments and datasets

A whole host of compatibility and consistency issues can make working with multi-sensor and multi-platform data a highly nontrivial and tedious endeavor (e.g., [53,54]). Therefore, we believe that one should resist the temptation to include in the mix all existing satellite aerosol datasets at the very outset irrespective of their real or imaginary virtues since this is likely to make the problem unphysical. A more realistic and productive approach would be to start with a minimal combination of datasets that are believed to be the most reliable and mutually consistent and can be expected to be sufficient for the solution of the problem in hand, at least in the first approximation. The other datasets should be invoked only if doing so proves to be necessary and appropriate.

The MODIS and MISR instruments onboard Terra launched in 1999 and the MODIS onboard Aqua launched in 2002 currently provide the most comprehensive remote sensing of tropospheric aerosols from space. Furthermore, the MODIS and MISR datasets are the most compatible ones in terms of their duration, spatial resolution, and spatial, temporal, and spectral overlap as well as in terms of their retrieval approaches and specific aerosol deliverables. Therefore, they naturally form the basis of the proposed framework.

Similarly, the NASA/GEWEX GACP dataset appears to be an appropriate means of extrapolating the new knowledge back in time and creating a multi-decadal aerosol climatology. Since the GACP record is based on two-channel aerosol retrievals and includes the Ångström exponent as well as the AOT, it is believed to be more consistent with the MODIS and MISR retrieval strategies than the operational one-channel NOAA product [30,55]. By the same token, the specific two-channel AVHRR retrieval methodology proposed in [56] differs from that adopted for MODIS and GACP and will not be considered here.

Another critical component of the proposed framework is the use of the benchmark data acquired with the RSP as well as the future Glory APS dataset. As always, an important validation tool is the AERONET dataset [57]. We also expect that data from other passive satellite instruments as well as from the CALIPSO lidar [58] may become important and useful at an advanced stage of creating the unified long-term aerosol climatology.

The brief summaries given below are intended to highlight the instrument and data characteristics essential for this study. Since the Glory APS is less known to the atmospheric community, its description will be more extensive than those of the other key instruments.

### 2.1. MODIS

MODIS-Terra (morning orbit) and MODIS-Aqua (afternoon orbit) have a viewing swath width of 2330 km and provide global coverage of the whole Earth every 1 to 2 days with a moderate spatial resolution (250–1000 m). Their detectors yield radiance measurements in 36 spectral bands ranging in wavelength from 400 to 14,400 nm, seven of which (nominal wavelengths 470, 550, 660, 870, 1240, 1640 and 2130 nm) are used for aerosol characterization. The strength of the MODIS instruments lies in the combination of wide spectral range, relatively high spatial resolution, and in-flight calibration of the visible and thermal IR channels [59]. The shortcomings are the inability to distinguish aerosol size distribution, type, and particle shape with radiance measurements alone and the use of the same visible radiances for both cloud screening and aerosol retrievals. A detailed description of the aerosol retrieval algorithm can be found in [32,60,61]. The operational MODIS aerosol product consists of the AOT, effective radius, and fine mode fraction retrieved over both land and the oceans. Based on extensive comparisons with AERONET data, it is claimed that one standard deviation of MODIS optical thickness retrievals fall within the predicted uncertainty of $\Delta\tau = \pm 0.03 \pm 0.05\,\tau$ over ocean and $\Delta\tau = \pm 0.05 \pm 0.15\,\tau$ over land, while one standard deviation of MODIS effective radius retrievals falls within $\Delta r_{\text{eff}} = \pm 0.11\,\mu\text{m}$ [32].

### 2.2. MISR

The MISR instrument consists of nine pushbroom cameras that view the Earth in nine different directions (four forward, four backward, and nadir) at four wavelengths (446, 558, 672, and 866 nm) and also includes in-flight radiance calibration [62]. It is claimed that combining MISR multi-wavelength and multi-angle radiance observations provide some ability to retrieve aerosol type and discriminate spherical and nonspherical particles. However, the MISR products are likely to be subject to cloud contamination, particularly by thin cirrus, since there are no suitable SWIR or thermal channels for cloud screening. MISR has a 360 km wide swath, thereby taking 9 days for complete global coverage. This means that monitoring of day-to-day aerosol variability is limited. The corresponding aerosol retrieval algorithms have been documented in [63,64]. The MISR product consists of the AOT, Ångström exponent, and aerosol type retrieved over both land and the oceans. The latter two aerosol characteristics are not yet available operationally as part of MISR level 3 data. It has been claimed [31] that overall, about $\frac{2}{3}$ of the MISR-retrieved AOT values fall within $\pm 0.05$ or $\pm 0.2\tau$ of AERONET, while more than a third are within $\pm 0.03$ or $\pm 0.1\tau$.

### 2.3. NASA/GEWEX GACP

The aerosol product generated under the NASA/GEWEX GACP consists of the AOT and Ångström exponent retrieved over the oceans from channel 1 and 2 AVHRR radiances [27]. The principal limitations of this product are the extremely limited spectral sampling used (630 and 865 nm) and the likely negative effects of imperfect cloud screening and calibration uncertainties [27,65–67]. However, the unique 25 year GACP record provides valuable information on potential trends in the spatial and temporal variability of atmospheric aerosols over the ocean. There is no pixel-level validation of the GACP retrievals with in situ measurements due to the limited number of cloud-free AVHRR pixels ($4 \times 4$ km resolution sampled to 30 km) contained in the gridded ISCCP DX dataset [54]. Nevertheless, statistical comparisons with ship-borne sun-photometer results have shown good agreement. It has been found that the ensemble-averaged GACP AOT overestimates the ensemble-averaged sun-photometer data only by about 3.6% with a random error of about 0.04 [36,42].

### 2.4. RSP

The RSP is an aircraft instrument developed for NASA in 1999 by SpecTIR Corporation. It allows the total and linearly polarized reflectances to be measured simultaneously in nine spectral channels for each IFOV [68]. This is accomplished by six boresighted telescopes that have the same IFOV of 14 mrad and provide simultaneous determination of the Stokes parameters $I$, $Q$, and $U$ in nine spectral channels with a wide

dynamic range (14-bit digitization) and high SNR (greater than 250 at radiance levels typical of aerosols over the ocean) with a radiometric and polarimetric uncertainty of $\leqslant 5\%$ and $\leqslant 0.2\%$, respectively.

The specific RSP measurement approach employs Wollaston prisms to make simultaneous measurements of orthogonal intensity components from the same scene. This ensures that the polarization signal is not contaminated by scene intensity variations during the course of the polarization measurements, which could create "false" or "scene" polarization. The nine RSP spectral bands are capable of sampling most of the spectral variations in reflected sunlight due to particle scattering in the atmosphere. That is, the 412-, 470-, and 555-nm reflectances are significantly affected by molecular scattering in addition to scattering by submicron and super-micron (including cloud) particles. The 672- and 865-nm reflectances, on the other hand, are predominantly caused by scattering due to sub-micron and super-micron particles, and the 1590-, 1880-, and 2250-nm reflectances by scattering due to super-micron particles only. The 960- and 1880-nm bands are sensitive to the amount of water vapor and to the presence of cirrus clouds, respectively. The 14 mrad IFOVs are continuously scanned by a polarization-neutral two-mirror system which allows 152 viewing-angle samples (with a dwell time of 1.875 ms for each sample) to be acquired over a $120^\circ$ angular range.

By performing highly accurate and precise, multi-angle, and multi-spectral measurements of polarization as well as intensity, RSP serves as a close proxy to an ultimate passive instrument for aerosol and cloud remote sensing. It takes full advantage of the extreme sensitivity of high-accuracy polarization data to aerosol and cloud particle microphysics and thereby enables the simultaneous retrieval of the parameters needed in the quantification of the direct and indirect aerosol effects [49–51]. The RSP has been used to collect extensive data during the CLAMS (http://www-clams.larc.nasa.gov/clams), CRYSTAL-FACE (http://cloud1.arc.nasa.gov/crystalface/), IHOP (http://www.eol.ucar.edu/dir_off/projects/2002/IHOP.html), CSTRIPE (http://www.cstripe.caltech.edu/links.html), ALIVE, and INTEX-B/MILAGRO (http://www.windows.ucar.edu/tour/link=/milagro/milagro_intro.html) field campaigns. These data are publicly available on-line at http://data.giss.nasa.gov/rsp_air/data_analysis.html.

### 2.5. *Glory APS*

The NASA Glory Mission will be flown as part of the A-train in a nominal 705-km altitude and $98.2^\circ$ inclination sun-synchronous polar orbit with a 1:34 pm equatorial crossing time and is scheduled for launch in December 2008.

The Glory APS design approach required to ensure high accuracy in polarimetric measurements follows that of RSP. As noted above, such measurements are not subject to "false" polarization resulting from time-sequential measurements of the polarization states and degrading the accuracy of polarization imagers such as POLDER [19]. To measure the complete set of Stokes vector elements that define the state of linear polarization ($I$, $Q$, and $U$), APS employs a pair of telescopes with one telescope measuring $I$ and $Q$ (polarization azimuths of $0^\circ$ and $90^\circ$) and the other telescope measuring $I$ and $U$ (polarization azimuths of $45^\circ$ and $135^\circ$). The resulting redundant measurement set increases the reliability of APS. The APS measurements of $I$, $Q$, and $U$ are similar to those provided by POLDER but with substantially better accuracy because of the unique spectral, spatial, and temporal simultaneity afforded by the specific APS design.

Dichroic beam splitters and interference filters define nine APS spectral channels centered at the wavelengths $\lambda = 410$, 443, 555, 670, 865, 910, 1370, 1610, and 2200 nm. Thus, the spectral range and its sampling provided by APS are similar to those used in MODIS aerosol retrievals [60]. All spectral channels but the 1370 nm one are free of strong gaseous absorption bands. The 1370 nm exception is centered at a major water vapor absorption band and is intended for detection and characterization of thin cirrus [69]. The spectral positions of the other eight channels are consistent with the optimized aerosol retrieval strategy. In particular, they take advantage of several natural circumstances such as the darkness of the ocean at longer wavelengths in the visible and near-infrared, the lower land albedo at shorter visible wavelengths, and the potential for using the 2200-nm channel to characterize the land surface contribution at visible wavelengths. The 910-nm channel will be used to determine the column water vapor amount.

The ability to view a scene from multiple angles is provided by scanning the APS IFOV along the spacecraft ground track with angular samples acquired every $8 \pm 0.4$ mrad. The APS polarization-compensated scanner assembly consists of a pair of matched mirrors operating in a "crossed" (orthogonal) configuration.

The corresponding viewing-angle range at the Earth surface is $+60/-80^\circ$ with respect to nadir. This overall range is similar to those provided by MISR and POLDER, but is scanned quasi-continuously ($\sim$250 view angles) rather than sampled at nine and 14 fixed directions, respectively.

APS has four calibration references that are viewed each scan. A dark reference uses a blackened light-trap cavity to provide a reference for zero illumination on each scan. A solar reference uses a Spectralon solar diffuser, which is illuminated during passage over the North pole on every orbit to define the radiometric calibration at the start of the Glory mission. An unpolarized reference uses a polarization scrambler to reduce the polarization of the nadir Earth scene to negligible, known levels that is viewed on every scan. Finally, a polarized reference uses crystal polarizers to polarize the nadir Earth scene to known levels close to 100% that is viewed each scan. Since the solar diffuser will degrade once it is illuminated by sunlight, the stability of the APS radiometric scale is ensured via monthly, same-phase lunar calibrations. The APS on-board references provide comprehensive tracking of polarimetric calibration throughout each orbit. The radiometric stability is tracked monthly to ensure that the aerosol and cloud retrieval products are stable over the period of the mission.

The unique APS design is intended to maximize the microphysical retrieval capability of the instrument (Table 1). As a consequence, APS is not an imager and provides no cross-track coverage beyond the width of its nominal IFOV. Also, the comparatively large size of the APS IFOV (5.6 km at nadir) can cause partial cloud contamination of many APS pixels (e.g., [70]). This problem will be mitigated by using two high-spatial-resolution cloud cameras and the cloud-screening algorithm developed in [71]. Additional approaches will be to (i) attempt the retrieval of both the cloud and the dominant aerosol mode within a partially cloudy pixel and (ii) exploit the fact that $Q$ and $U$ become insensitive to subpixel cloudiness at scattering angles $\lesssim 140^\circ$.

### 2.6. AERONET

AERONET is a globally dispersed network of automated ground-based sun/sky scanning radiometers, which provides correlative ground-based measurements for satellite and model validation studies at specific geographic locations [57]. Typically, the AOT uncertainty of AERONET measurements is estimated to be about $\pm 0.01$ to $\pm 0.02$, with larger spectrally dependent errors ($\pm 0.02$) in the UV spectral range [57,72]. The accuracy of AERONET-retrieved SSAs is estimated to be within 0.03 [73]. Because of their relatively high AOT accuracy, AERONET data are widely used in the validation of satellite retrievals and transport-model results. The multi-modal size distribution, refractive index, and shape are also part of the AERONET product. The principal limitation of the AERONET dataset is that with a restricted number of stations unevenly

Table 1
Flowdown of APS measurement characteristics into specific retrieval capabilities

| Measurement characteristic | Retrieval capability |
|---|---|
| Precise polarimetry ($\sim$0.1%) | Particle size distribution, refractive index, and shape |
| Wide scattering angle range for both intensity and polarization | Particle size distribution, refractive index, and shape |
| Multiple ($\gtrsim$20) viewing angles for both intensity and polarization | (i) Cloud particle size via rainbow angle<br>(ii) Particle size distribution, refractive index, and shape<br>(iii) Ocean surface roughness |
| Multiple ($\gtrsim$20) viewing angles + precise polarimetry | Aerosol retrievals in cloud-contaminated pixels |
| Wide spectral range (400–2200 nm) for both intensity and polarization | (i) Separation of submicron and supermicron particles<br>(ii) Spectral refractive index $\Rightarrow$ chemical composition |
| 1370 nm channel for both intensity and polarization | Detection and characterization of thin cirrus clouds |
| 2200 nm polarization channel | Characterization of the land surface contribution at visible wavelengths |
| 910 nm channel | Column water vapor amount |

distributed across the globe, the measurements may not be sufficiently dense for global coverage, especially over the oceans. Also, it is unclear how the assumption that all components of the multi-modal aerosol population have the same refractive index affects the retrieval of the size distribution.

## 3. Comparative analysis of MODIS, MISR, and GACP datasets

As we have mentioned in the preceding section, the development of the unified aerosol climatology should start with a comprehensive comparative analysis of the MODIS, MISR, and GACP aerosol products. Fig. 5 shows time series of the global AOT and Ångström exponent for MODIS-Terra, MODIS-Aqua, MISR, and AVHRR (GACP) for the full period of contemporaneously available data. MODIS level 3 collection 004 monthly mean quality assured data as well as the latest publicly available level 3 MISR data were used in the comparison. Also shown are MODIS-Aqua collection 005 retrieval results. The closest agreement (differences in AOT $\lesssim 0.03$) is found between the MODIS-Terra and MODIS-Aqua data. This is not surprising given the instrument and algorithm similarity. The MISR AOT values are the largest of the four instruments (greater than the MODIS AOTs by 0.03–0.04). Strong Asian dust storms are responsible for the AOT spike in 2003. This event is especially apparent in the MODIS-Aqua time series but was screened out by the GACP cloud detection algorithm.

The comparison of the Ångström exponent series (the MISR Ångström exponent data were not available at the time of writing) shows a more complex picture. There are significant differences in the global Ångström exponent values, up to 0.3, between the two MODIS instruments. The GACP-derived Ångström exponent values are generally in between those retrieved by the two MODIS instruments. A change of data quality is apparent in the GACP record in 2001. However, the reason for a sudden large change in the MODIS-Terra record in 2001 needs to be further explored. Also, an upward trend in the Ångström exponent noticeable in the MODIS-Terra data may be an indication of a stability problem in one of the spectral channels. The MODIS-Aqua collection 005 Ångström-exponent retrievals are significantly lower than the collection 004 MODIS-Aqua results. This may potentially be attributed to changes in the refractive index in some of the aerosol optical models used in the retrieval algorithm.

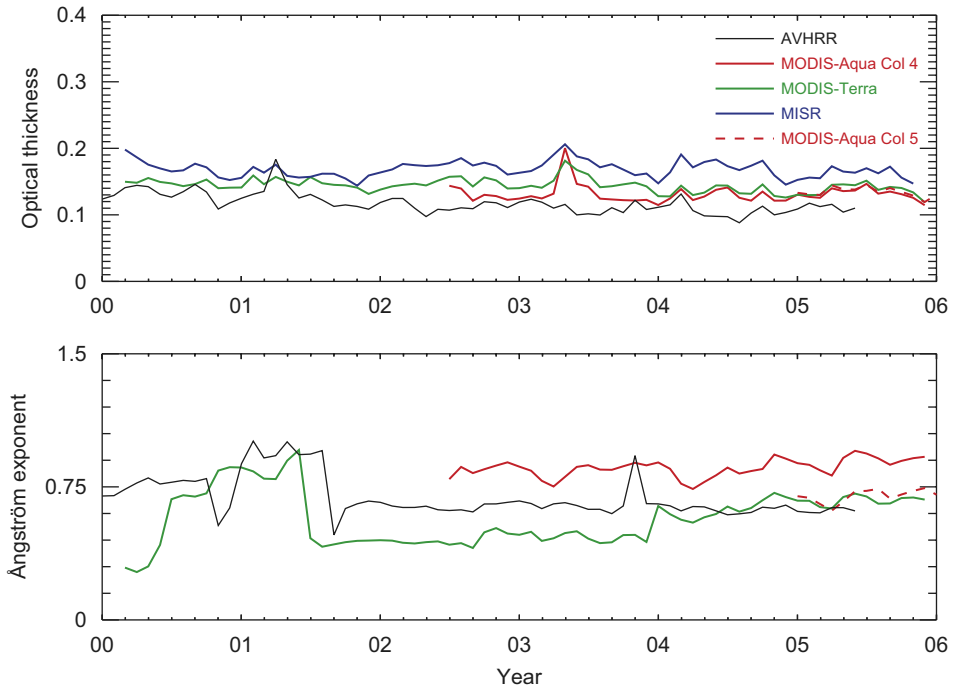


Fig. 5. Time series of the global mean values of the AOT (top panel) and Ångström exponent (bottom panel) over the oceans.

Fig. 5 quantifies the overall current discrepancies between the global aerosol climatologies. A number of factors can contribute to the observed differences, of which the major ones are different cloud masks, calibration, aerosol model assumptions, and surface reflectance models (e.g., [27,40]). In order to separate and quantify the effects of these factors, we need to compare retrievals on smaller scales. One way to achieve this is to compare retrievals for regions with different characteristic aerosol types, as discussed next.

Figs. 6 and 7 show scatter plots of MODIS-Terra, MODIS-Aqua, and MISR AOTs for three regions: Persian Gulf, Southern Pacific Ocean between the 0° and 40°S latitudes, and the 40–60°S latitudinal belt. Each point in the plots represents a monthly mean AOT further averaged over a $10^\circ \times 10^\circ$ box within the borders of a given region. All comparisons are shown for the same period between 07/2002 and 06/2005 during which data from all four instruments were available. These three regions were selected because they are dominated by distinctly different aerosol types (cf. [67]). In the compact Persian Gulf region, high loads of desert dust aerosol are regularly observed, while the Southern Pacific Ocean is representative of a clean maritime aerosol environment. The 40–60°S belt is characterized by elevated amounts of sea salt aerosol due to high surface winds.

In the Persian Gulf region, the two MODIS instruments agree rather well in terms of AOT (see the left-hand top panel of Fig. 6). A larger spread in the AOT values is observed in the Southern Pacific and within the 40–60°S belt. Very large statistical discrepancies with a strong systematic component are observed between the Ångström exponent values retrieved by the MODIS-Aqua and MODIS-Terra instruments in all three regions (see the right-hand column of Fig. 6). On average, the MODIS-Terra underestimates the Ångström exponent relative to the MODIS-Aqua by about 0.3 in the Persian Gulf region and by as much as 0.7 in the Southern Pacific. Since the two instruments and the corresponding retrieval algorithms are essentially identical, the significant Ångström-exponent differences may be indicative of a calibration problem in one of the channels or a systematic dependence on the illumination–viewing geometry as the two instruments view the same area at different times.

The MISR AOTs are systematically greater than the MODIS-Aqua ones in the Southern Pacific and in the 40–60°S belt, but can be significantly smaller in the Persian Gulf region (Fig. 7). In addition to the monthly mean AOT values, the right-hand column of Fig. 7 compares the corresponding seasonal averages. If the discrepancies observed in the left-hand column were due to the different sampling of the MODIS and MISR instruments, one would expect a reduction in the statistical spread in the seasonal averages compared to the monthly averages. The obvious absence of such a reduction indicates that the discrepancies are inherent to the underling retrieval procedures.

Fig. 8 compares MODIS-Aqua collection 004 and 005 monthly $10^\circ \times 10^\circ$ retrievals for the same three regions for the year 2005. In general, the two algorithms produce similar AOTs with regression gains close to unity and small intercept values. The best agreement between the two versions of AOT is found in the Persian Gulf region, where aerosol loads are high. There is a much greater spread of data points in the Ångström-exponent plots. The Collection 004 Ångström exponents are systematically greater than the Collection 005 results, potentially due in part to the changes in the refractive index in some aerosol models used in the newer retrievals. The largest spread is observed in the Southern Pacific region, where small aerosol loads strengthen the effect of surface and atmosphere parameter estimates on the retrieval results. Interestingly, the MOIDS-Aqua Collection 005 Ångström exponent values are much closer to the MODIS-Terra Collection 004 values. However, to fully assess the consequences of the algorithm upgrade, we must wait until MODIS-Terra Collection 005 data become available.

It is clear that the regional comparisons of the aerosol products yield significantly more information on the distribution and potential origin of the differences between the MODIS and MISR datasets. However, to gain the best understanding of the strengths and limitations of these aerosol data sets one ultimately needs to examine pixel-level retrievals, in which case the influence of many more parameters can be analyzed. It is, therefore, necessary to use contemporaneous and collocated MODIS and MISR level 2 data to analyze in detail select orbits and areas. This will allow one to achieve the following goals.

Analyze the influence of specific cloud-masking algorithms on the average retrieved aerosol parameters. Sensitivity studies and our previous experience with the GACP dataset ([27]; see also [29,70,71]) indicate that cloud screening can be an important source of errors in the retrieved AOT and aerosol size parameters. The relative impact of sub-pixel cloud contamination and subvisible cirrus can be estimated by investigating

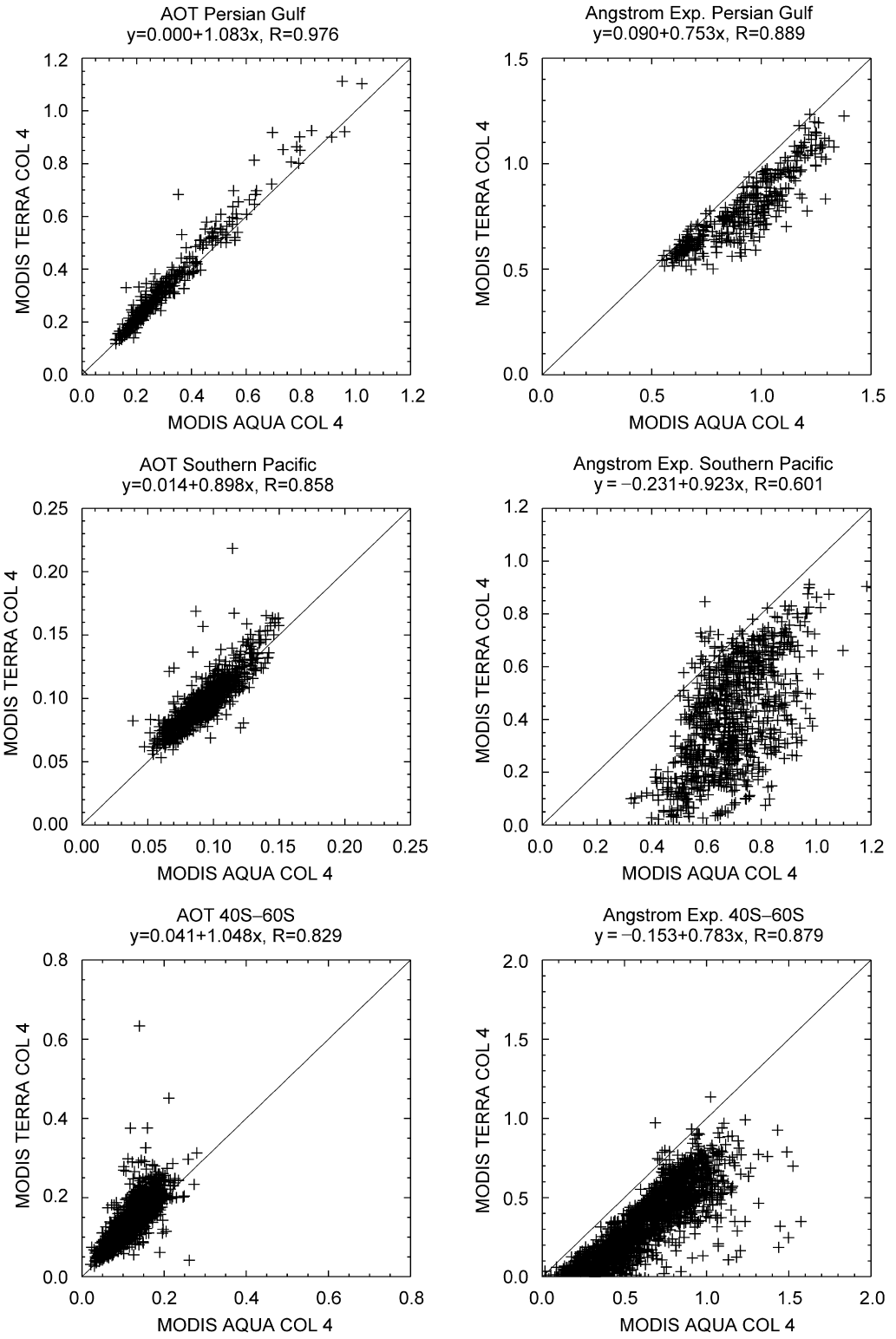


Fig. 6. MODIS-Terra vs. MODIS-Aqua scatter plots.

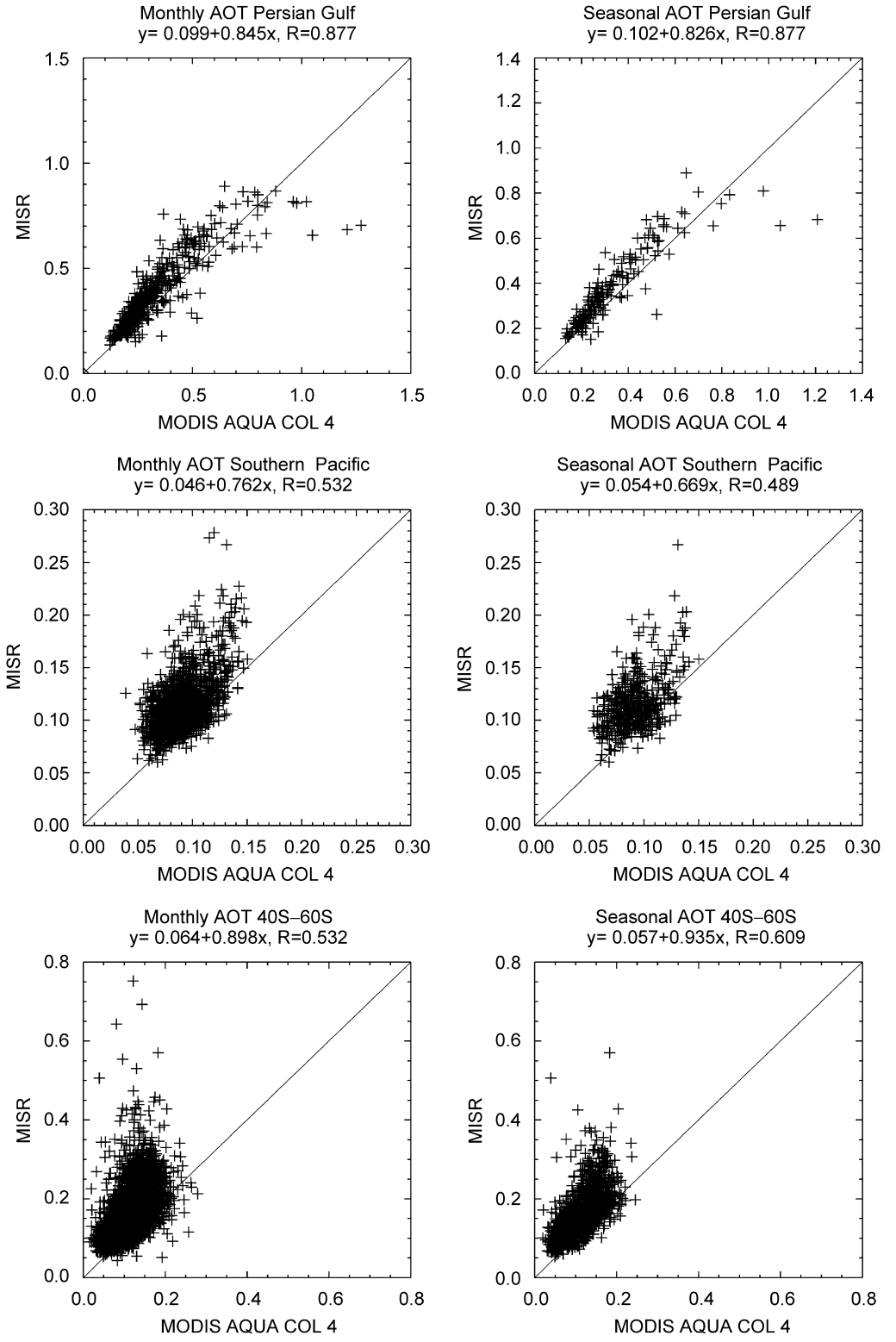


Fig. 7. MODIS-Aqua vs. MISR scatter plots.

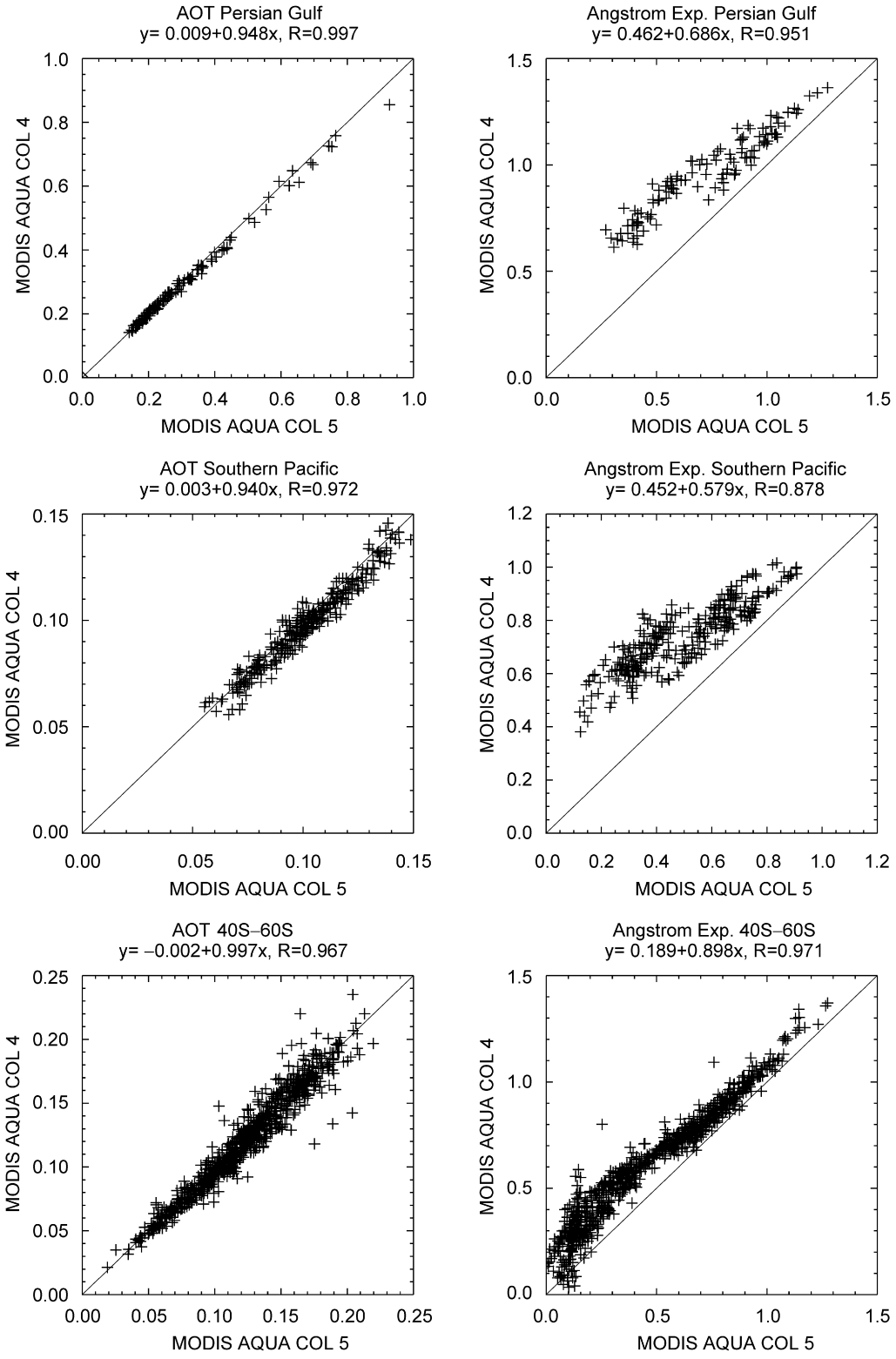


Fig. 8. Collection 004 vs. collection 005 MODIS-Aqua scatter plots.

the dependence of differences in the retrieved AOTs on the cloud amount supplemented by pixel-by-pixel comparisons of cloud/no-cloud decisions made by the MODIS and MISR cloud screening procedures.

Study the relative radiometric stability of the instruments by looking at carefully selected clean remote maritime regions over the period of several years.

Compare aerosol products in areas dominated by maritime aerosols (e.g., Southern Hemisphere midlatitudes), which will allow one to investigate the combined influence of sea-surface reflection assumptions and aerosol optical models on the retrievals.

Look for and analyze any differences in the aerosol seasonal cycle for regions where a strong cycle is present such as areas influenced by desert dust outflows, biomass burning, and wind pattern changes. The results should be compared with AERONET data. Special attention should be paid to the cases in which a significant fraction of aerosol can be expected to be mineral dust [74]. The nonsphericity of dust particles can have a profound effect on the retrieval results [75–81]. Therefore, one should analyze specifically whether there is a systematic effect of the MODIS scattering angle on the differences between the MODIS and MISR retrievals.

## 4. Use of RSP and APS data

To get further insight into the detailed behavior of the MODIS and MISR retrieval algorithms and evaluate the accuracy of the retrieval results, it would be extremely instructive to perform extensive comparisons of MODIS and MISR results with aerosol retrievals from RSP data collected during the field experiments listed in Section 2.4. As we have already mentioned, the RSP can provide direct proxy datasets for the MODIS and MISR measurements and can thus be used to perform a detailed step-by-step analysis of the MODIS and MISR retrieval procedures (e.g., [49]). At the same time, the RSP polarimetric data are much more sensitive to the aerosol particle microphysics and optical thickness and thus will enable one to identify the specific causes of failures in the MODIS and MISR retrievals. Many flights of RSP during these field experiments were specifically designed to coincide with MODIS and MISR overpasses. Furthermore, the RSP data have been collected in a variety of environments and are thus representative of the majority of aerosol types sampled by MODIS and MISR observations, including the morphologically complex dust and soot particles [75,82]. The unique ability of the RSP to retrieve the aerosol particle microphysics can be used to develop specific recommendations for the improvement and extension of the range of particle models used in the MODIS and MISR look-up tables. A previous example of using RSP results to improve MISR retrievals was documented in [83].

Other critical advantages of RSP measurements are their sensitivity to the presence and properties of optically thin cirrus clouds and to the liquid-droplet size distribution. These factors can help to quantify the potential effect of sub-visible cirrus clouds on the MISR aerosol retrievals and further test MODIS and MISR cirrus and liquid-cloud retrievals. Also, the availability of polarimetric measurements in the 2250 nm band enables the RSP retrieval algorithm to yield accurate AOTs over land, which can help to quantify the errors in the MODIS and MISR retrievals caused by surface reflectance uncertainties.

An ultimate test of the MODIS and MISR aerosol climatologies on the global scale will become available after the launch of the Glory mission. It is likely that the quality and accuracy of the APS retrievals will be lower than those of the RSP retrievals due to a significantly larger size of the APS IFOV. Still, it is reasonable to expect that the APS retrievals will be far superior to the MODIS and MISR ones and can serve as a global benchmark with coverage and data volume greatly exceeding those of the AERONET, especially over the vast ocean areas.

We expect that the result of such research will be a much better understanding of the nature of the MODIS and MISR aerosol climatologies as well as of their respective accuracies and areas of applicability. It will also allow one to formulate a set of specific recommendations and recipes on how to improve the existing MODIS and MISR retrieval algorithms.

## 5. Use of MODIS and MISR datasets to improve the GACP product

We have already mentioned that in the framework of the NASA/GEWEX GACP, the ISCCP-calibrated channel 1 and -2 AVHRR radiances have been used to develop a global climatology of the column AOT and

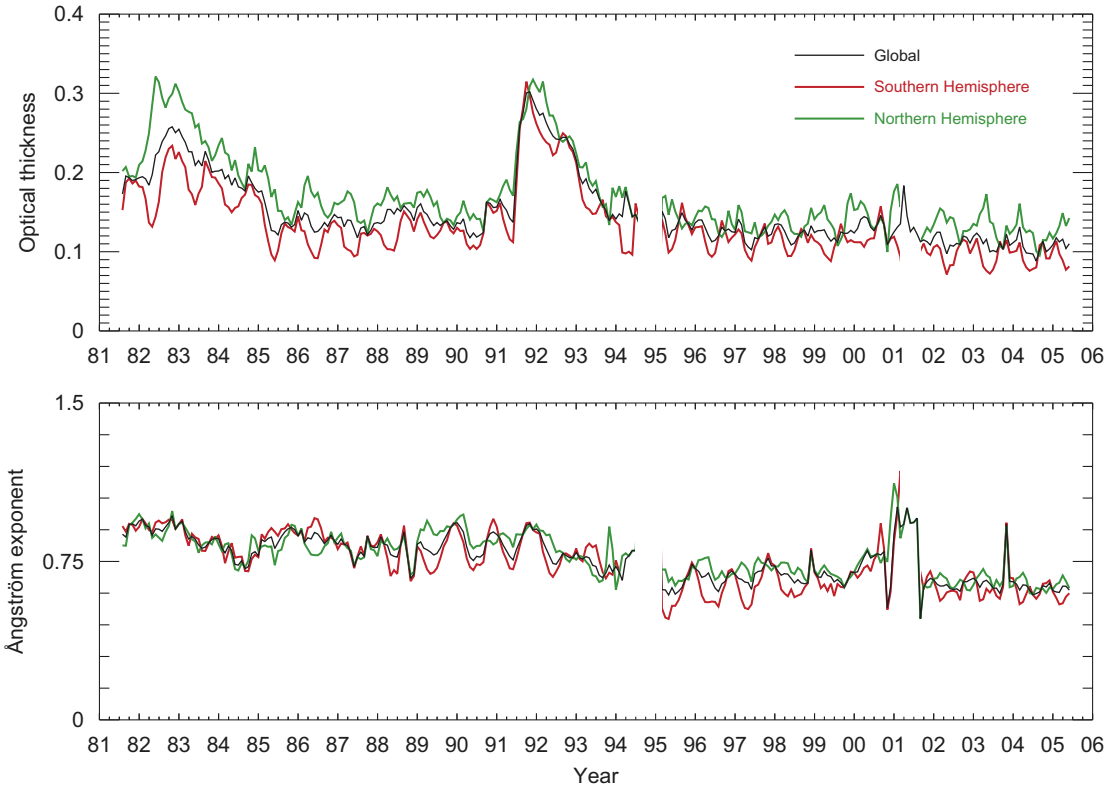


Fig. 9. Global and hemispherical monthly averages of the AOT and Ångström exponent for the period August 1981–June 2005.

Ångström exponent over the oceans for the period August 1981–June 2005 (http://gacp.giss.nasa.gov). Fig. 9 demonstrates the long-term behavior of the global monthly mean AOT and Ångström exponent. With only two pieces of data per pixel available, the GACP algorithm has an extremely limited retrieval capability and must rely on many a priori assumptions with regard to the numerous parameters of the atmosphere–surface system other than the AOT and Ångström exponent [27]. The absence of an on-board radiance calibrator serves to further exacerbate the problem. The GACP AOT dataset has been tested versus ship-borne sun-photometer results [36,42], and the way these tests were designed served to check simultaneously the radiance calibration, the performance of the cloud-screening algorithm, and the accuracy of AOT retrievals. However, the ultimate test of the GACP retrieval algorithm must be based on global comparisons with improved MODIS and MISR aerosol products. Indeed, this will enable one to put additional constraints on the a priori assumptions used in the GACP retrieval algorithm in order to make them more realistic in terms of their global applicability. Comparisons of coincident GACP and MODIS/MISR retrievals can help to assess the accuracy of the former on the global to regional scale, which is not currently possible with AERONET measurements alone. Specifically, the operation of MODIS and MISR instruments since early 2000 presents a unique opportunity to:

(i) evaluate and improve the GACP calibration of channel-1 and -2 AVHRR radiances,
(ii) validate and improve the GACP cloud-screening algorithm,
(iii) compare the GACP aerosol product to those generated from the MODIS and MISR data,
(iv) apply the GACP cloud screening and aerosol retrieval algorithms to sampled MODIS radiances and compare the result with the equivalent MODIS product,
(v) evaluate the information content of the extra spectral channels on MODIS and similar radiometers,
(vi) reprocess the entire GACP radiance dataset and derive an improved aerosol product, and

(vii) merge the GACP aerosol product with the MODIS and MISR records, thereby enhancing the value of these newer datasets without having to wait for another 20 years.

The AVHRR calibration issue should be addressed in concert with the parallel ISCCP effort and should take advantage of the fact that the aerosol tests provide more sensitivity to the intercept than most other indirect calibration methods.

For illustration, Figs. 10 and 11 parallel Figs. 6–8, but compare MODIS-Aqua/MISR and GACP retrievals. The GACP AOT is lower than the MODIS-Aqua AOT over the dust-dominated Persian Gulf region and somewhat lower in the Pacific with large statistical spread, which is expected given the low quality of the AVHRR radiance data. The comparison of the respective Ångström exponents (Fig. 11) shows that while the average values are similar in magnitude, the GACP algorithm has problems in clean maritime environments due to low signal-to-noise ratio. Somewhat unexpectedly, however, the Ångström exponent differences between the GACP and MODIS-Aqua retrievals can be significantly smaller than those between the MODIS-Aqua and MODIS-Terra retrievals, as comparison of Figs. 11 and 6 reveals.

## 6. Synthesis of MODIS, MISR, and GACP climatologies

To integrate the satellite aerosol products into a coherent and consistent climatology is a very difficult task. Indeed, it is reasonable to expect that even after repeated revisions of the MODIS and MISR retrieval algorithms there will still be significant differences between the respective aerosol products caused by inherent differences in the sensitivity of MODIS and MISR radiances to the various parameters of the atmosphere–surface system. For example, the MISR radiances will never have adequate sensitivity to the presence of sub-visible cirrus clouds, whereas the MODIS radiances will never be directly indicative of the presence of nonspherical particles. Thus, the integration of the MODIS and MISR products cannot be expected to be a straightforward and well-defined procedure. Instead, one may think of several ways of combining these products, and the approach giving the best results in one application may not suite another application.

Perhaps, the most conservative approach is to limit the spatial and temporal coverage to that of MISR and include in the combined climatology only those pixels that are declared cloud free by both cloud-screening algorithms and are assigned the same AOT by both retrieval algorithms. Although this approach may be expected to be the most reliable, it is likely to result in a rather small number of pixels (especially in areas dominated by dust-like aerosols and areas with frequent occurrence of thin cirrus clouds) and may not help much in studies of short-term regional trends. There are multiple ways to relax this conservative approach, including those based on giving preference to either MODIS or MISR results depending on the type of environment or even on a unified retrieval algorithm using as input radiance-level data from both MODIS and MISR, and it is not clear at this time which one of them will prove to be the most appropriate. Therefore, instead of committing oneself to a specific approach at the outset, one should examine as many different approaches as possible and select the most appropriate one(s) at the very end.

After the differences between the MODIS and MISR products have been reconciled to the extent possible, the use of the integrated product in the improvement of the GACP algorithm should be rather straightforward. It will then be possible to add the fully re-processed GACP dataset to the combined MODIS–MISR product, thereby yielding a unified three-decade-long aerosol climatology which is expected to find numerous applications.

One immediate application might be to compare the SAGE and improved GACP results obtained for the periods affected by major volcanic eruptions. The two most important events easily identifiable in the GACP record (Fig. 9) are the El Chichon (March 1982) and Mt. Pinatubo (June 1991) eruptions. No eruptions of comparable magnitude have been observed with the more advanced instruments such as MODIS, MISR, and POLDER, which emphasizes the importance of the historic satellite data in studies of the climatic effects of such major perturbations. The SAGE instruments provided quasi-direct measurements of the optical thickness of stratospheric aerosols during and after these eruptions. However the spatial coverage of the SAGE measurements is rather sparse due to the nature of occultation observations. The GACP data provide estimates of the total column AOT and Ångström exponent in the climatically important visible spectral

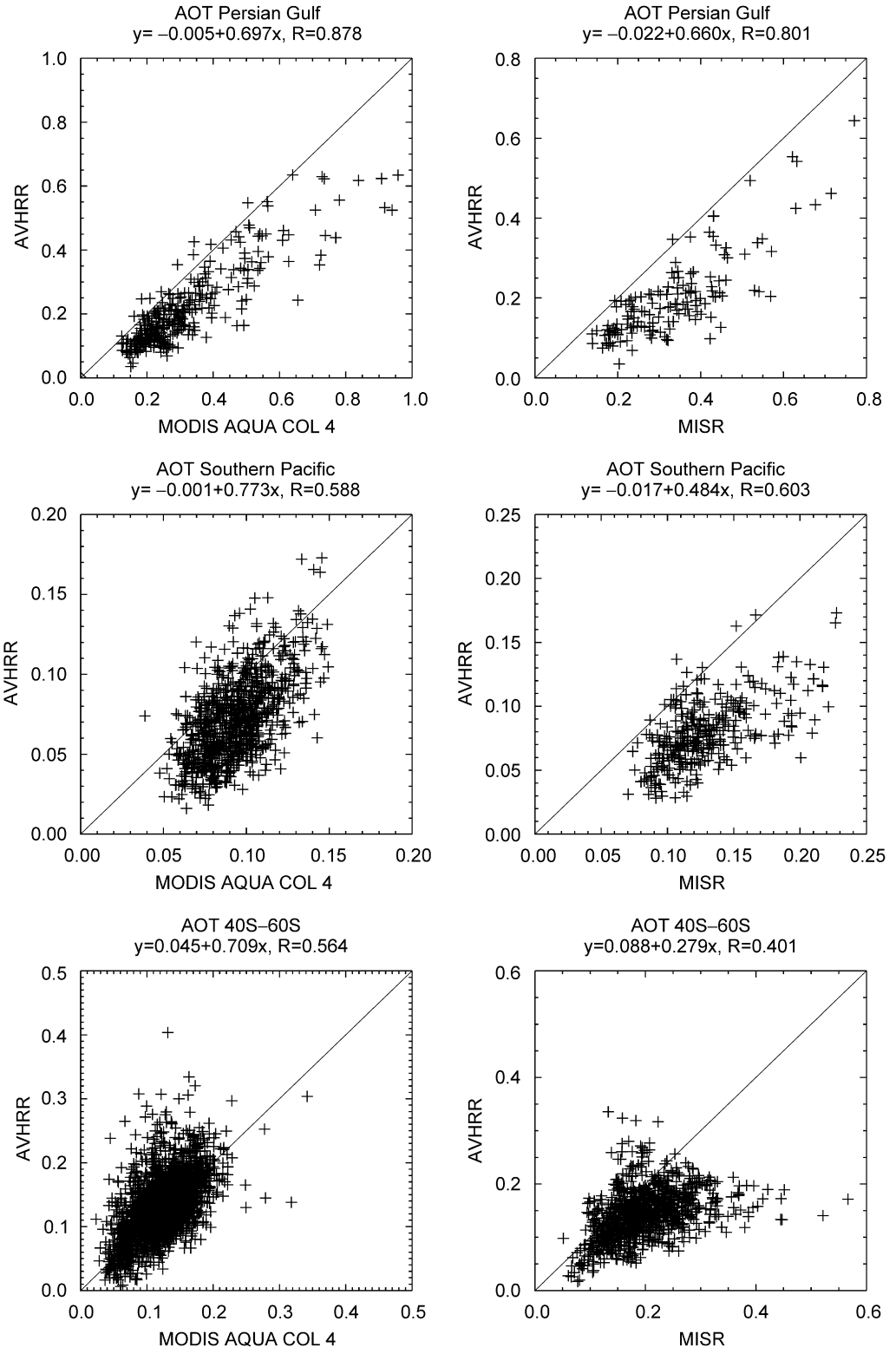


Fig. 10. MODIS-Aqua/MISR vs. GACP scatter plots of AOT.

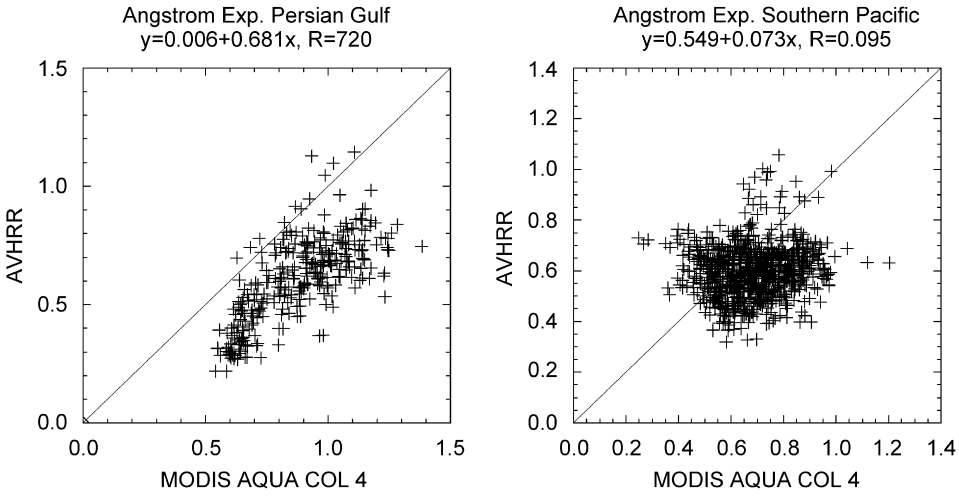


Fig. 11. MODIS-Aqua versus GACP Ångström-exponent scatter plots.

region with significantly better spatial resolution than the SAGE data. Geogdzhayev et al. [66] showed that it is possible to separate the stratospheric and tropospheric aerosol components in the GACP retrieval by using the SAGE data as an auxiliary input and to create a time series of tropospheric aerosols. Alternatively one can calculate the climatologically mean tropospheric aerosol load using eruption-free periods before and after the eruptions. One can then subtract the mean tropospheric AOT from the column GACP AOT to create a time series of volcanic aerosols for the period affected by the eruptions. This will allow one to track the spatial and temporal distribution of the volcanic aerosol and estimate the aerosol removal time. The GACP product can be validated by using the SAGE zonal mean values and compared with the contemporaneous TOMS aerosol index product.

## 7. Discussion and conclusions

The integrated science data analysis approach described above is envisaged to yield the following specific results:

(i) The quantification of the accuracy and likely limits of applicability of each satellite dataset.
(ii) The clarification of the meaning, accuracy, and utility of various spatial and/or temporal averages (including global and annual averages) of aerosol characteristics.
(iii) The clarification of the extent to which the various satellite datasets are coherent, complimentary, and/or contradictory.
(iv) The rationalization of specific improvements in the existing MODIS, MISR, and GACP aerosol retrieval algorithms and in the future VIIRS algorithms.
(v) A meaningful synthesis of the MODIS, MISR, and GACP aerosol products into a three-decade-long global climatology.

One can thus expect that the outcome of this research will (i) advance our understanding of the factors that determine atmospheric concentrations of aerosols, (ii) provide an improved description of the global distributions of aerosols and their radiative properties, (iii) reduce the uncertainty regarding the direct and indirect effects of the changing distributions of aerosol, and (iv) provide a more definitive observational foundation to evaluate decadal- to century-scale variability and change.

The combined analysis of MODIS, MISR, and APS retrievals should also help define a more accurate and definitive framework for the formulation of a comprehensive space mission intended to fully and accurately address the extremely complex aerosol forcing problem. Irrespective of potential improvements to the MODIS and MISR retrieval algorithms, these instruments will never yield all the aerosol and cloud characteristics and

the respective accuracies listed in the right-hand panel of Fig. 2. The APS, on the other hand, is a close proxy to the ultimate passive instrument discussed in Section 1 and does yield the requisite retrieval capability along the ground track but lacks the cross-track coverage characteristic of imaging instruments. It would thus appear that building and flying an imaging polarimeter would solve the problem once and for all.

Unfortunately, the impressive performance of the aircraft version of APS, viz., the RSP, and the growing recognition of polarimetry as an indispensable tool for solving the aerosol-forcing problem from space has led to a tendency to trivialize the notion of a polarimeter as an aerosol remote-sensing instrument. Increasingly often one encounters proposals of polarization-sensitive imagers characterized as being ''similar to APS only better'', the adjective ''better'' referring to the imaging capability. One should keep in mind, however, that RSP and APS yield the requisite retrieval capability only owing to the unique combination of their specific measurement characteristics. Therefore, the only acceptable solution would be to have an instrument that has the same measurement characteristics as APS as well as the imaging capability (this is well demonstrated by Table 1, which illustrates the impact of dropping a specific APS measurement capability on the resulting retrieval capability). Unfortunately, such an instrument is extremely difficult to build in general and in the form of an affordable space-qualified design in particular. This is especially true of ensuring high polarimetric accuracy which seems to be incompatible with having the imaging capability (all existing imaging polarimeters appear to have polarimetric accuracy $\sim$2% or worse; see, e.g., the review [84]).

It may thus turn out that the only feasible solution would be to fly a synergistic combination of APS and a state-of-the-art imaging polarimeter such as the advanced POLDER (POLDER-A) currently under development (Didier Tanré, personal communication). The POLDER-A is a multi-channel multi-angle imaging photopolarimeter which has essentially all the measurement characteristics of APS except the high polarimetric accuracy and can provide aerosol and cloud retrievals with a 2-day global coverage. The APS, on the other hand, can provide in-flight calibration of POLDER-A polarimetry, benchmark aerosol and cloud retrievals along the satellite ground track, and improved and updated look-up tables for the POLDER-A cross-track retrievals.

## Acknowledgment

This research was funded by the NASA Radiation Sciences Program managed by Donald Anderson and Hal Maring and by the NASA Glory Mission project.

## References

[1] Ramaswamy V, et al. Radiative forcing of climate change. In: Houghton JT, et al., editors. Climate change 2001: the scientific basis. Cambridge: Cambridge University Press; 2001. p. 349–416.
[2] Loeb NG, Manalo-Smith N. Top-of-atmosphere direct radiative effect of aerosols over global oceans from merged CERES and MODIS observations. J Climate 2005;18:3506–26.
[3] Lohmann U, Feichter J. Global indirect aerosol effects: a review. Atmos Chem Phys 2005;5:715–37.
[4] Bates TS, et al. Aerosol direct radiative effects over the northwest Atlantic, northwest Pacific, and North Indian Oceans: estimates based on in-situ chemical and optical measurements and chemical transport modeling. Atmos Chem Phys 2006;6:1657–732.
[5] Schulz M, et al. Radiative forcing by aerosols as derived from the AeroCom present-day and pre-industrial simulations. Atmos Chem Phys 2006;6:5225–46.
[6] Penner JE, et al. Model intercomparison of indirect aerosol effects. Atmos Chem Phys 2006;6:3391–405.
[7] Yu H, et al. A review of measurement-based assessments of the aerosol direct radiative effect and forcing. Atmos Chem Phys 2006;6:613–66.
[8] Hansen J, et al. Earth's energy imbalance: confirmation and implications. Science 2005;308:1431–5.
[9] Hansen J, et al. Efficacy of climate forcings. J Geophys Res 2005;110:D18104.
[10] Schwartz SE. Uncertainty requirements in radiative forcing of climate change. J Air Waste Manage Assoc 2004;54:1351–9.
[11] Diner DJ, et al. PARAGON: an integrated approach for characterizing aerosol climate impacts and environmental interactions. Bull Am Meteorol Soc 2004;85:1491–501.
[12] Seinfeld JH, et al. Scientific objectives, measurement needs, and challenges motivating the PARAGON aerosol initiative. Bull Am Meteorol Soc 2004;85:1503–9.
[13] Mishchenko MI, et al. Monitoring of aerosol forcing of climate from space: analysis of measurement requirements. JQSRT 2004;88:149–61.

[14] King MD, Kaufman YJ, Tanré D, Nakajima T. Remote sensing of tropospheric aerosols from space: past, present, and future. Bull Am Meteorol Soc 1999;80:2229–59.
[15] Torres O, et al. A long-term record of aerosol optical depth from TOMS observations and comparison to AERONET measurements. J Atmos Sci 2002;59:398–413.
[16] Torricella F, et al. Retrieval of aerosol properties over the ocean using global ozone monitoring experiment measurements: method and applications to test cases. J Geophys Res 1999;104:12085–98.
[17] Carboni E. GOME aerosol optical depth retrieval over ocean: correcting for the effects of residual cloud contamination. Atmos Environ 2006;40:6975–87.
[18] Wang M, Bailey S, McClain CR. SeaWiFS provides unique global aerosol optical property data. EOS Trans Am Geophys Union 2000;81:197.
[19] Deschamps P-Y, et al. The POLDER mission: instrument characteristics and scientific objectives. IEEE Trans Geosci Remote Sens 1994;32:598–615.
[20] King MD, et al. Cloud and aerosol properties, precipitable water, and profiles of temperature and water vapor from MODIS. IEEE Trans Geosci Remote Sens 2003;41:442–58.
[21] Diner DJ, et al. Multi-angle imaging spectroradiometer (MISR) instrument description and experiment overview. IEEE Trans Geosci Remote Sens 1998;36:1072–87.
[22] Chylek P, Henderson B, Mishchenko M. Satellite based retrieval of aerosol optical thickness: the effect of sun and satellite geometry. Geophys Res Lett 2003;30:1533.
[23] Veefkind JP, de Leeuw G, Stammes P, Koelemeijer RBA. Regional distribution of aerosol over land, derived from ATSR-2 and GOME. Remote Sens Environ 2000;74:377–86.
[24] Grey WMF, North PRJ, Los SO, Mitchell RM. Aerosol optical depth and land surface reflectance from multiangle AATSR measurements: global validation and intersensor comparisons. IEEE Trans Geosci Remote Sens 2006;44:2184–97.
[25] Torres O, Decae R, Veefkind P, de Leeuw G. OMI aerosol retrieval algorithm. In: Stammes P, editor. OMI algorithm theoretical basis document, clouds, aerosols and surface UV irradiance, vol. 3. Utrecht: Royal Netherlands Meteorological Institute; 2002. p. 47–71.
[26] Gottwald M, et al. SCIAMACHY—monitoring the changing Earth's atmosphere. Weßling, Germany: DLR Institut für Methodik der Fernerkundung; 2006.
[27] Mishchenko MI, et al. Aerosol retrievals over the ocean by use of channels 1 and 2 AVHRR data: sensitivity analysis and preliminary results. Appl Opt 1999;38:7325–41.
[28] Higurashi A, et al. A study of global aerosol optical climatology with two-channel AVHRR remote sensing. J Climate 2000;13: 2011–27.
[29] Ignatov A, Nalli NR. Aerosol retrievals from multi-year multi-satellite AVHRR Pathfinder Atmosphere (PATMOS) dataset for correcting remotely sensed sea surface temperatures. J Atmos Oceanic Technol 2002;19:1986–2008.
[30] Stowe LL, et al. The advanced very high resolution radiometer (AVHRR) pathfinder atmosphere (PATMOS) climate dataset: initial analyses and evaluations. J Climate 2002;15:1243–60.
[31] Kahn R, et al. Multiangle imaging spectroradiometer (MISR) global aerosol optical depth validation based on 2 years of coincident aerosol robotic network (AERONET) observation. J Geophys Res 2005;110:D10S04.
[32] Remer LA, et al. The MODIS aerosol algorithm, products and validation. J Atmos Sci 2005;62:947–73.
[33] Liu L, et al. Assessing Goddard Institute for Space Studies ModelE aerosol climatology using satellite and ground-based measurements: a comparison study. J Geophys Res 2006;111:D20212.
[34] Kinne S, et al. Monthly averages of aerosol properties: a global comparison among models, satellite data, and AERONET ground data. J Geophys Res 2003;108:4634.
[35] Yu H, et al. Annual cycle of global distributions of aerosol optical depth from integration of MODIS retrievals and GOCART model simulations. J Geophys Res 2003;108:4128.
[36] Liu L, et al. Global validation of two-channel AVHRR aerosol optical thickness retrievals over the oceans. JQSRT 2004;88: 97–109.
[37] Myhre G, et al. Intercomparison of satellite retrieved aerosol optical depth over the ocean. J Atmos Sci 2004;61:499–513.
[38] Myhre G, et al. Intercomparison of satellite retrieved aerosol optical depth over ocean during the period September 1997 to December 2000. Atmos Chem Phys 2005;5:1697–719.
[39] Myhre G, et al. Comparison of the radiative properties and direct radiative effect of aerosols from a global aerosol model and remote sensing data over ocean. Tellus B 2007;59:115–29.
[40] Jeong M-J, Li Z. Quality, compatibility, and synergy analyses of global aerosol products derived from the advanced very high resolution radiometer and total ozone mapping Spectrometer. J Geophys Res 2005;110:D10S08.
[41] Jeong M-J, Li Z, Chu DA, Tsay S-C. Quality and compatibility analyses of global aerosol products derived from the advanced very high resolution radiometer and moderate resolution imaging spectroradiometer. J Geophys Res 2005;110:D10S09.
[42] Smirnov A, et al. Ship-based aerosol optical depth measurements in the Atlantic Ocean: comparison with satellite retrievals and GOCART model. Geophys Res Lett 2006;33:L14817.
[43] Mishchenko MI, Travis LD. Satellite retrieval of aerosol properties over the ocean using measurements of reflected sunlight: effect of instrumental errors and aerosol absorption. J Geophys Res 1997;102:13543–53.
[44] Mishchenko MI, Travis LD. Satellite retrieval of aerosol properties over the ocean using polarization as well as intensity of reflected sunlight. J Geophys Res 1997;102:16989–7013.
[45] Hansen JE, Travis LD. Light scattering in planetary atmospheres. Space Sci Rev 1974;16:527–610.

[46] Mishchenko MI, Travis LD, Lacis AA. Scattering, absorption, and emission of light by small particles. Cambridge: Cambridge University Press; 2002 (available in the PDF format at http://www.giss.nasa.gov/~crmim/books.html).
[47] Hovenier JW, van der Mee C, Domke H. Transfer of polarized light in planetary atmospheres—basic concepts and practical methods. Dordrecht, The Netherlands: Kluwer Academic Publishers; 2004.
[48] Mishchenko MI, Travis LD, Lacis AA. Multiple scattering of light by particles: radiative transfer and coherent backscattering. Cambridge: Cambridge University Press; 2006.
[49] Chowdhary J, Cairns B, Mishchenko M, Travis L. Retrieval of aerosol properties over the ocean using multispectral and multiangle photopolarimetric measurements from the research scanning polarimeter. Geophys Res Lett 2001;28:243–6.
[50] Chowdhary J, Cairns B, Travis LD. Case studies of aerosol retrievals over the ocean from multiangle, multispectral photopolarimetric remote sensing data. J Atmos Sci 2002;59:383–97.
[51] Chowdhary J, et al. Retrieval of aerosol scattering and absorption properties from photopolarimetric observations over the ocean during the CLAMS experiment. J Atmos Sci 2005;62:1093–117.
[52] Hasekamp OP, Landgraf J. Retrieval of aerosol properties over the ocean from multispectral single-viewing-angle measurements of intensity and polarization: retrieval approach, information content, and sensitivity study. J Geophys Res 2005;110:D20207.
[53] Rossow WB, Schiffer RA. ISCCP cloud data products. Bull Am Meteorol Soc 1991;71:2–20.
[54] Rossow WB, Schiffer RA. Advances in understanding clouds from ISCCP. Bull Am Meteorol Soc 1999;80:2261–87.
[55] Zhao TX-P, et al. Development of a global validation package for satellite oceanic aerosol optical thickness retrieval based on AERONET observations and its application to NOAA/NESDIS operational aerosol retrievals. J Atmos Sci 2002;59:294–312.
[56] Ignatov A, Stowe L. Aerosol retrievals from individual AVHRR channels. Part I: Retrieval algorithm and transition from Dave to 6S radiative transfer model. J Atmos Sci 2002;59:313–34.
[57] Holben BN, et al. AERONET—a federated instrument network and data archive for aerosol characterization. Remote Sens Environ 1998;66:1–16.
[58] Poole LR, Winker DM, Pelon JR, McCormick MP. CALIPSO: global aerosol and cloud observations from lidar and passive instruments. Proc SPIE 2003;4881:419–26.
[59] Xiong X, Che N, Barnes W. Terra MODIS on-orbit spatial characterization and performance. IEEE Trans Geosci Remote Sens 2005;43:355–65.
[60] Tanré D, Kaufman YJ, Herman M, Mattoo S. Remote sensing of aerosol properties over oceans using the MODIS/EOS spectral radiances. J Geophys Res 1997;102:16971–88.
[61] Levy RC, et al. Evaluation of the moderate-resolution imaging spectroradiometer (MODIS) retrievals of dust aerosol over the ocean during PRIDE. J Geophys Res 2003;108:8594.
[62] Kahn R, et al. MISR calibration and implications for low-light-level aerosol retrieval over dark water. J Atmos Sci 2005;62:1032–52.
[63] Martonchik JV, et al. Determination of land and ocean reflective, radiative, and biophysical properties using multiangle imaging. IEEE Trans Geosci Remote Sens 1998;36:1266–81.
[64] Kahn R, Banerjee P, McDonald D. The sensitivity of multiangle imaging to natural mixtures of aerosols over ocean. J Geophys Res 2001;106:18219–38.
[65] Geogdzhayev IV, et al. Global two-channel AVHRR retrievals of aerosol properties over the ocean for the period of NOAA-9 observations and preliminary retrievals using NOAA-7 and NOAA-11 data. J Atmos Sci 2002;59:262–78.
[66] Geogdzhayev IV, Mishchenko MI, Liu L, Remer L. Global two-channel AVHRR aerosol climatology: effects of stratospheric aerosols and preliminary comparisons with MODIS and MISR retrievals. JQSRT 2004;88:47–59.
[67] Geogdzhayev IV, et al. Regional advanced very high resolution radiometer-derived climatology of aerosol optical thickness and size. J Geophys Res 2005;110:D23205.
[68] Cairns B, Russell EE, LaVeigne JD, Tennant PMW. Research scanning polarimeter and airborne usage for remote sensing of aerosols. Proc SPIE 2003;5158:33–44.
[69] Gao B-C, Kaufman YJ. Selection of the 1.375 μm MODIS channel for remote sensing of cirrus clouds and stratospheric aerosols from space. J Atmos Sci 1995;52:4231–7.
[70] Henderson BG, Chýlek P. The effect of spatial resolution on satellite aerosol optical depth retrieval. IEEE Trans Geosci Remote Sens 2005;43:1984–90.
[71] Martins JV, et al. MODIS cloud screening for remote sensing of aerosols over oceans using spatial variability. Geophys Res Lett 2002;29. doi:10.1029/2001GL013252.
[72] Eck TF, et al. Wavelength dependence of the optical depth of biomass burning, urban, and desert dust aerosols. J Geophys Res 1999;104:31333–49.
[73] Dubovik O, et al. Variability of absorption and optical properties of key aerosol types observed in worldwide locations. J Atmos Sci 2002;59:590–608.
[74] Reid JS, et al. Comparison of size and morphological measurements of coarse mode dust particles from Africa. J Geophys Res 2003;108:8593.
[75] Mishchenko MI, Travis LD, Kahn RA, West RA. Modeling phase functions for dustlike tropospheric aerosols using a shape mixture of randomly oriented polydisperse spheroids. J Geophys Res 1997;102:16831–47.
[76] Mishchenko MI, et al. Aerosol retrievals from AVHRR radiances: effects of particle nonsphericity and absorption and an updated long-term global climatology of aerosol properties. JQSRT 2003;79/80:953–72.
[77] Krotkov NA, et al. Effect of particle nonsphericity on satellite monitoring of drifting volcanic ash clouds. JQSRT 1999;63:613–30.
[78] Zhao TX-P, et al. A study of the effect of non-spherical dust particles on the AVHRR aerosol optical thickness retrievals. Geophys Res Lett 2003;30:1317.

[79] Wang J, et al. The effects of non-sphericity on geostationary satellite retrievals of dust aerosols. Geophys Res Lett 2003;30:2293.
[80] Dubovik O, et al. The application of spheroid models to account for aerosol particle non-sphericity in remote sensing of desert dust. J Geophys Res 2006;111:D11208.
[81] Horvath H, Kasahara M, Tohno S, Kocifaj M. Angular scattering of the Gobi Desert aerosol and its influence on radiative forcing. J Aerosol Sci 2006;37:1287–302.
[82] Liu L, Mishchenko MI. Effects of aggregation on scattering and radiative properties of soot aerosols. J Geophys Res 2005;110:D11211.
[83] Martonchik JV, Diner DJ, Crean KA, Bull MA. Regional aerosol retrieval results from MISR. IEEE Trans Geosci Remote Sens 2002;40:1520–31.
[84] Tyo JS, Goldstein DL, Chenault DB, Shaw JA. Review of passive imaging polarimetry for remote sensing applications. Appl Opt 2006;45:5453–69.